Journal of Hazardous Materials 176 (2010) 193–198

Contents lists available at ScienceDirect

Journal of Hazardous Materials

journal homepage: www.elsevier.com/locate/jhazmat

Effective removal of selenate from aqueous solutions by the Friedel phase

Yueying Wu[a], Ying Chi[a], Hongmei Bai[a], Guangren Qian[a,*], Yali Cao[a], Jizhi Zhou[b], Yunfeng Xu[a], Qiang Liu[a], Zhi Ping Xu[b,**], Shizhang Qiao[b]

[a] School of Environmental and Chemical Engineering, Shanghai University, Shanghai 200072, PR China
[b] ARC Centre of Excellence for Functional Nanomaterials, Australian Institute for Bioengineering and Nanotechnology and School of Engineering, The University of Queensland, Brisbane, QLD 4072, Australia

ARTICLE INFO

Article history:
Received 1 April 2009
Received in revised form 3 November 2009
Accepted 3 November 2009
Available online 10 November 2009

Keywords:
Friedel phase
Layered double hydroxide
Selenate
Fixation
Hydrocalumite

ABSTRACT

This research has demonstrated that the Friedel phase, e.g. a chloride-containing hydrocalumite ($Ca_2Al(OH)_6Cl(H_2O)_2{\cdot}mH_2O$), can rapidly adsorb large amounts of SeO_4^{2-} (up to 1.37 mmol/g). SeO_4^{2-} is removed via anionic exchange, as evidenced by the expansion of the d-spacing from 0.78 nm of Cl-hydrocalumite to 0.97–0.98 nm of SeO_4-hydrocalumite. The newly formed SeO_4-adsorbed hydrocalumite is stable in water at pH 4–13, indicating the strong fixation of selenate within the phase. In contrast, intercalated selenate in the Freidel phase can be recovered by desorbing in the NaCl solution, which can also regenerate and recycle the used adsorbent. The findings in this research strongly suggest that the Friedel phase is a new, environmentally friendly and cost-effective adsorbent to adsorb selenate from wastewater streams and dilute solutions.

© 2009 Elsevier B.V. All rights reserved.

1. Introduction

Selenium, existing mainly in selenate and selenite in wastewater streams, is recognized as a severe environmental and health hazard as it is toxic to all living organisms and has a long half life (about 10^5 years) with high mobility within the eco-environmental system. Letey et al. reported that 10 ppb of selenate (SeO_4^{2-}) in water can cause death and birth deformities of waterfowls [1]. For this reason, the U.S. EPA set up the primary drinking-water standard to be 0.01 mg(Se)/l [2]. However, many anthropogenic activities, such as agricultural irrigation with drainage water and various mining and oil refinery effluents (170–4900 μg/l) [3], result in selenate and selenite entering the environment and water systems. Therefore, removal of selenium from wastewater streams is urgently needed [4].

The current strategy is to adsorb the selenate/selenite with various adsorbents to form precipitates and thus immobilize the selenate/selenite [5–13]. Hence, the key issue is to devise a suitable immobilizing phase to fix a high amount of selenate/selenite via adsorption, exchange, and/or oxidation–reduction, such as using designed adsorbent to remove various heavy metals [14,15]. A number of adsorbents have been investigated with the removal capacity mostly ranging from 0.1 to 0.81 mmol/g (Table 1), where hydrocalumite is most cost-effective. Further, interest in hazardous waste treatment processes using hydrocalumite has grown steadily in the past few years [16]. Hydrocalumite ($[Ca_2(Al,Fe)(OH)_6]^+X^-{\cdot}mH_2O$, denoted as AFm conventionally) has the same lamellar structure as natural hydrotalcite, where X^- is an anion, such as OH^-, Cl^-, SO_4^{2-}, and CO_3^{2-}. Hydrotalcite-like compounds, known as layered double hydroxides (LDHs), are a family of anionic clay minerals consisting of cationic brucite-like layers and exchangeable interlayer anions, and most can be nominally expressed as a chemical formula $[M_{1-x}^{2+}M_x^{3+}(OH)_2]^{x+}(A^{n-})_{x/n}{\cdot}mH_2O$, where M^{2+} represents any divalent metal cation, M^{3+} any trivalent metal cation and A^{n-} an anion (inorganic or organic) [17]. Due to their unique properties, LDHs and their derived materials have found many potential applications in water treatment [17–19]. In particular, MgAl–Cl–LDH, ZnAl–Cl–LDH, ZnFe–SO_4–LDH were used to adsorb selenate/selenite, showing that LDHs are a potential effective adsorbent for selenate/selenite [6,12].

In this study, hydrocalumite was selected for the following reasons. Firstly, hydrocalumite (AFm) mainly occurs in the hydrated cement paste, and thus can be cheaply prepared. Secondly, hydrocalumite immobilizes various metal oxyanions, such as chromate and arsenate [20–27]. Chrysochoou and Dermatas [23] established that AFm is more suitable than ettringite (AFt–SO_4) for oxyanion immobilization. Finally, some studies have demonstrated that the cement hydrate products (AFm–SO_4, AFt–SO_4, C–S–H etc.) can adsorb SeO_4^{2-}, but AFm–SO_4 (sulfate hydrocalumite) is more effective [24–26], involving the substitution of SO_4^{2-} with SeO_4^{2-} in

* Corresponding author. Tel.: +86 21 56338094; fax: +86 21 56333052.
** Corresponding author. Tel.: +61 7 33463809; fax: +61 7 33463973.
E-mail addresses: grqian@shu.edu.cn (G. Qian), gordonxu@uq.edu.au (Z.P. Xu).

0304-3894/$ – see front matter © 2009 Elsevier B.V. All rights reserved.
doi:10.1016/j.jhazmat.2009.11.012

Table 1
The adsorption capacities of selenate onto different adsorbents ($[SeO_4^{2-}]$ = 0–10 mM).

Sorbent	Capacity (mmol/g)	Reference
Mg_2Al–Cl–LDH	~0.3	[12]
Mg_4Al–Cl–LDH	~0.25	[12]
Zn_2Al–Cl–LDH	~0.3	[12]
Mg_2Al–SO_4–LDH	~0.1	[6]
Zn_2Fe–SO_4–LDH	~0.2	[6]
Fe/NN-MCM-41	0.81	[40]
Functionalized zeolite	0.002	[5]
Cuprite	0.012	[10]
Aluminum-oxide-coated sand	0.012	[7]
Friedel phase (AFm–Cl)	1.37	This study

the sorption mechanism [20–22,27]. In particular, the Friedel phase AFm–Cl ($Ca_2Al(OH)_6Cl(H_2O)_2{\cdot}mH_2O$, chloride hydrocalumite) is a major hydration product found in concrete submerged in seawater, which is subjected to Cl^- corrosion. As Cl^- has a less affinity for hydrocalumite than SO_4^{2-} and CO_3^{2-}, it is believed that the ion substitution of Cl^- with SeO_4^{2-}, e.g., adsorption of SeO_4^{2-}, takes place more easily. Qian et al. [28] established that Cl-rich MSWI fly ash can effectively stabilize chromate in the co-disposal of Cr-bearing industrial sludge via the formation of chromate–AFm. Hence, in this research, our aim was to investigate the adsorption–desorption behaviors of SeO_4^{2-} over the Friedel phase (AFm–Cl) in aqueous solution. We examined the fixation property of selenate on the Friedel phase and the chemical stability of the selenate–AFm products, and sought to understand the mechanism of SeO_4^{2-} adsorption/fixation on the Friedel phase.

2. Materials and methods

2.1. Chemicals

Alumina (Al_2O_3, AR grade), sodium chloride (NaCl, AR grade), calcium oxide (CaO, AR grade), calcium chloride ($CaCl_2{\cdot}6H_2O$, GA grade) and calcium hydroxide ($Ca(OH)_2$, GA grade) were purchased from Riedel-dehaen. Sodium selenate (Na_2SeO_4, 98%) and 1,5-diphenylcarbazid ($C_{13}H_{14}N_4O$, PA grade) were purchased from Fluka and Merck, respectively. All chemicals were used as received.

2.2. Mineral synthesis and characterization

The Friedel phase (AFm–Cl) was prepared by co-precipitation following the method reported previously [29]. In brief, 22 mmol of powdered $3CaO{\cdot}Al_2O_3$ (prepared at 1400 °C in our lab) was slowly added to a solution containing 22 mmol of $CaCl_2{\cdot}6H_2O$ (GA, Riedel-dehaen) under vigorous stirring. The mixed suspension was aged at 45 °C for 24 h under stirring. The precipitate was then collected via filtration, thoroughly washed with deionized water and dried at 100 °C in an oven.

The synthesized AFm–Cl was identified with the powder X-ray diffraction pattern recorded on a D8-X-Ray Diffractometer (Bruler, Germany) using Cu Kα radiation (λ = 0.15418 nm), and further characterized with the FTIR spectrum collected on a PerkinElmer GX50905 FT-IR spectrophotometer in the range of 4000–400 cm^{-1}, with a resolution of 4 cm^{-1} using the KBr pellet technique. The morphological images of the as-prepared Friedel phase were recorded on a scanning electron microscope (JSM-6360). The specific surface area was derived from the N_2 adsorption isotherm measured at 77 K on a Quantachrome NOVA-1200 gas absorption analyzer using the BET equation. In addition, Se was determined using a PerkinElmer Optima DV 2000 ICP–MS system and the chloride concentration was analyzed in a Flow Injection Analyzer (Lachat Quikchem8000) following the method in the literature [30].

2.3. Adsorption

To examine the adsorption kinetics, three Na_2SeO_4 aqueous solutions were prepared at $[SeO_4^{2-}]$ = 0.25, 1.25 and 5.00 mM. In each adsorption experiment, the initial solution pH was adjusted at 8 ± 0.05, and 0.10 g of Friedel phase was added to 50 ml of each solution with constant shaking (150 rpm) in a Yorco thermostatic shaking water bath. At the selected time intervals, 1.0 ml of aliquot liquid sample was withdrawn and centrifuged. The SeO_4^{2-} concentration in aqueous solution was determined with ICP–MS.

The isotherm adsorption experiments were carried out at room temperature while the initial concentration of SeO_4^{2-} ranged from 0.25 to 7.60 mM. After 2-h adsorption, the mixture was filtered through a G-4 crucible (Borosil), and the residual SeO_4^{2-} concentration in the filtrate was determined with ICP–MS.

All the experiments were carried out in duplicate with the reproducibility within ±5%, and the average values were reported in this paper. The pH was monitored using an Elico digital pH meter (Model LI-120) and a combined glass electrode (Model CL 51).

2.4. Desorption experiment

The Se-adsorbed AFm sample for desorption experiments was prepared by suspending 2.0 g of AFM–Cl in 1.0 l of 7.60 mM Na_2SeO_4 solution with the initial pH at 8 ± 0.05 with shaking at 150 rpm for 24 h. After drying in a vacuum, the collected solid sample (0.1 g) was added to 50 ml of aqueous solution containing 0.01, 0.02, 0.05 or 0.10 M NaCl to desorb selenate from the Se-adsorbed AFm. At selected time intervals, 1.0 ml sample was withdrawn to analyze the release amount of selenate with ICP–MS.

2.5. Chemical stability

For this test the Se-containing AFm was prepared by suspending 2.0 g of AFm–Cl in 1.0 l of 0.60 mM Na_2SeO_4 solution with the initial pH at 8 ± 0.05 and shaking at 150 rpm for 24 h. After drying in a vacuum, the Se-containing AFm (containing 0.280 mmol(Se)/g) was added to water with pH adjusted to 4 ± 0.05, 7 ± 0.05, 10 ± 0.05, or 13 ± 0.05 with 1.0 M HCl or NaOH, and the liquid/solid mass ratio set at 20:1 in accordance with the US toxicity characteristic leaching procedure (TCLP) [31]. At the selected time points (1, 2, 3, 4, 8, 16, and 24 h), the concentration of leached selenate was determined with ICP–MS.

3. Results and discussion

3.1. Physicochemical features of the Friedel phase

The synthesized AFm–Cl is a white powder. The SEM image (Fig. 1) shows that the crystallites have a hexagonal-plate form, with a lateral dimension of 0.2–3.0 μm. The specific surface area is 10.3 m^2/g and the interparticle pore size is distributed from 3.5 to 4.5 nm.

The XRD pattern (Fig. 2A) of the as-synthesized compound is in excellent agreement with that recorded on PDF 78–1219 in the database of the International Center for Diffraction Data, which suggests that the synthesized compound is typical of the Friedel phase, with a nominal chemical formula of $Ca_4Al_2(OH)_{12}Cl_2(H_2O)_4$. The cell parameters a = 0.993 nm, b = 0.573 nm and c = 1.595 nm, calculated from the diffraction peaks, are identical to those reported on PDF 78–1219.

The FTIR spectrum of the synthesized compound is shown in Fig. 2B. The strong overlapping bands at 3480 and 3636 cm^{-1} are attributed to the stretching vibrations of lattice water and structural OH groups (ν_{OH}) in the Friedel phase layer, respectively. The H–O–H bending vibration of the interlayer water molecule (ν_2 H_2O)

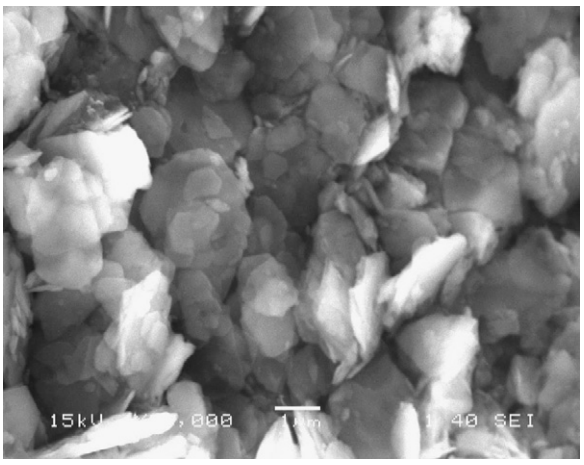

Fig. 1. SEM micrograph of the as-prepared Friedel phase (AFm–Cl).

is also reflected by the peak at 1621 cm^{-1}. The peak at 785 cm^{-1} is due to a stretching vibration of Al–OH (ν_1 Al–OH) and that at 532 cm^{-1} to a bending vibration of Al–OH (ν_3 Al–OH) [29]. In addition, the peak at 1442 cm^{-1} could be assigned to the anti-symmetric stretching vibration of CO_3^{2-} that was transferred from CO_2 captured from air during the AFm–Cl preparation. No vibration peaks of chloride ions appear in the range of 400–4000 cm^{-1} due to the ionic nature of the chloride bonding with the positive charge layer [29].

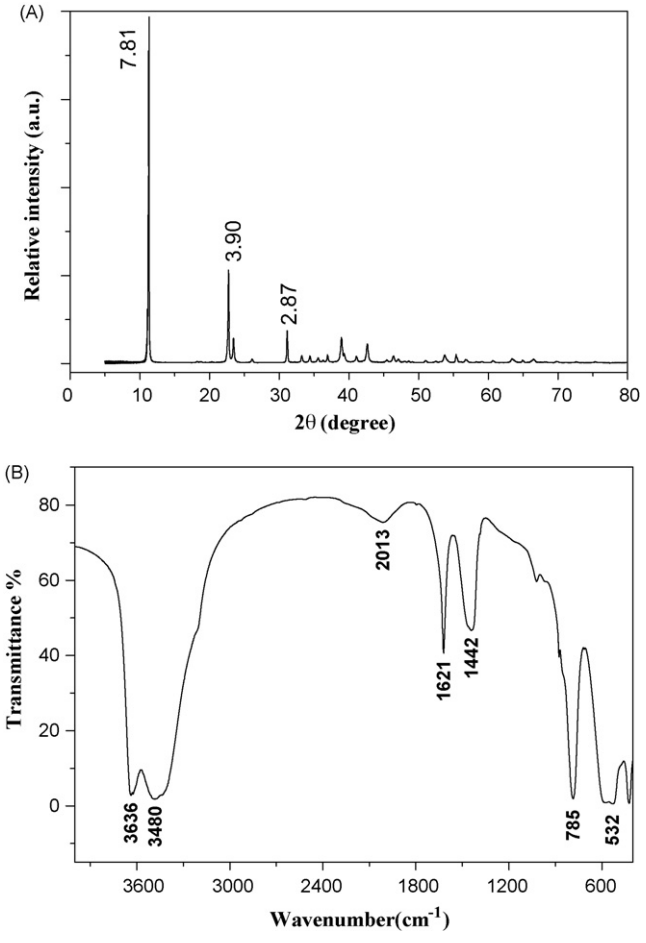

Fig. 2. (A) Powder XRD pattern of the as-prepared Friedel phase (AFm–Cl); (B) FTIR spectrum of the as-prepared Friedel phase.

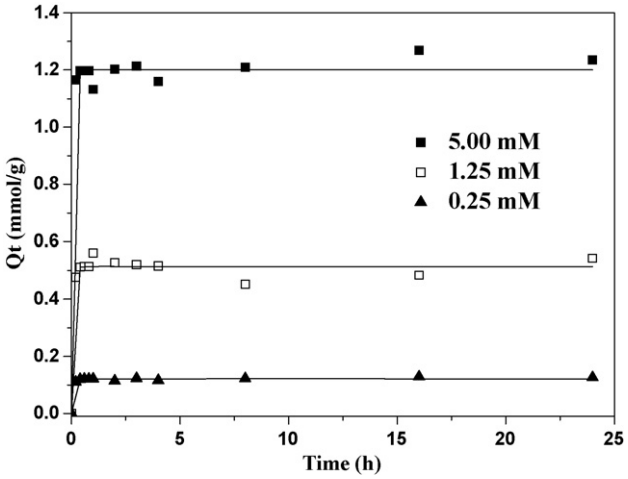

Fig. 3. Adsorption profile of SeO_4^{2-} on the Friedel phase (AFm–Cl).

3.2. Removal of selenate using the Friedel phase

As shown in Fig. 3, the selenate removal is a quick process, mainly occurring within the first ten minutes. The rapid removal can be attributed to the ion exchange mechanism [32], similar to the ion exchange process in soils and clay minerals [33]. After 1 h, the exchange seems to reach equilibrium. Similarly, the released Cl^- is quick in the first hour, but increased with time in all cases (Fig. 4), showing the continuity of the SeO_4^{2-}–Cl^- and/or CO_3^{2-}–Cl^- exchange process.

The selenate removal amount after 1 h is 0.12, 0.51 and 1.20 mmol/g (Se) at the initial $[SeO_4^{2-}]$ = 0.25, 1.25 and 5.00 mM, representing 98%, 82% and 48% removal of selenate from solution, respectively. The low removal percentage (48%) at $[SeO_4^{2-}]$ = 5.00 mM is due to the excess selenate added in the solution (5.00 mmol in 1 l) because 2.0 g of AFm–Cl in 1 l of solution can at most take up 3.56 mmol SeO_4^{2-} if we suppose AFm–Cl has a chemical formula of $Ca_4Al_2(OH)_{12}Cl_2(H_2O)_4$ (MW = 561).

Fig. 5 shows the isotherm for selenate exchange into the Friedel phase at 298 K. The highest removal amount under the current conditions is 1.37 mmol/g at the initial $[SeO_4^{2-}]$ = 7.60 mM. Considering the contamination of CO_3^{2-} and the water adsorption on the adsorbent AFm–Cl used in the experiment, this capacity is quite close to the theoretical exchange capacity of AFm–Cl (1.78 mmol/g). Such an exchange capacity of AFm is also higher than the other LDH materials and adsorbents reported elsewhere, as listed in Table 1. It is worthy mentioning that the initial pH (4–10) does not obviously affect the adsorption isotherm of selenate because pH jumps to above 10 in a minute and reaches to a value of 10.5–12.0 [34] (Supplementary material Fig. 1S).

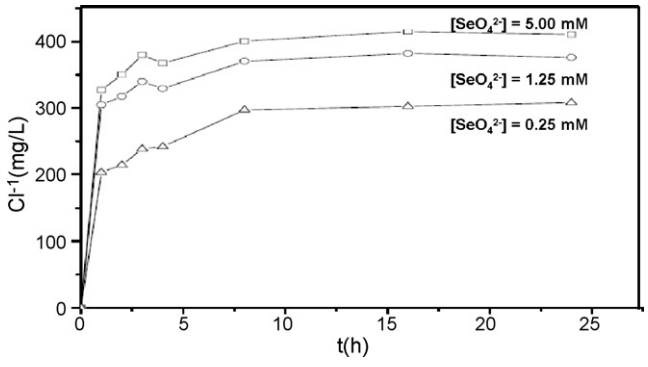

Fig. 4. The profile of Cl^- released from the Freidel phase during the selenate removal.

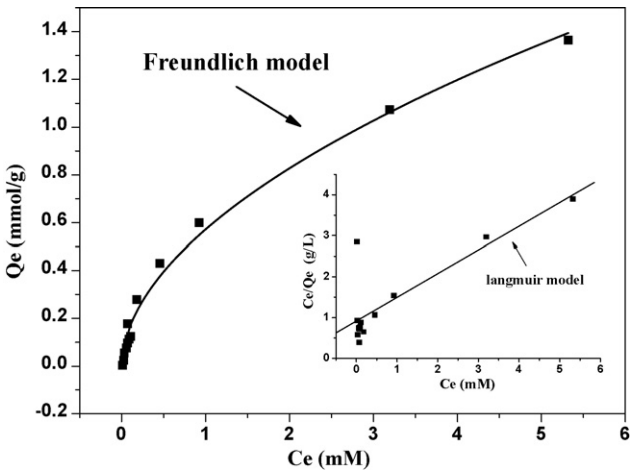

Fig. 5. Adsorption isotherm of SeO_4^{2-} on the as-prepared Friedel phase fitted with the Freundlich model and the Langmuir model (inset).

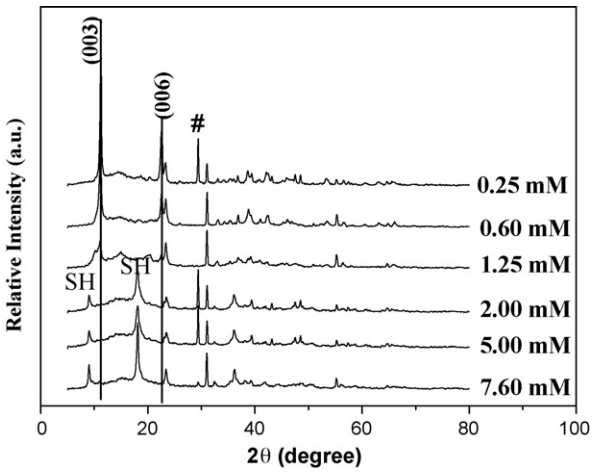

Fig. 6. XRD patterns of the Friedel phase adsorbed/intercalated with SeO_4^{2-} at various initial concentrations. Selenate-hydrocalumite phase is marked with 'SH', and $CaCO_3$ with '#'.

3.3. Removal mechanism over the Friedel phase

As proposed for the hydrotalcite-like adsorbents, the selenate removal involves both surface and interlayer anion exchange, as follows:

$$Ca_4Al_2(OH)_{12}(H_2O)_4\text{–}Cl_{2(surface)} + SeO_4^{2-} \Leftrightarrow Ca_4Al_2(OH)_{12}(H_2O)_4\text{–}SeO_{4(surface)} + 2Cl^- \quad (1)$$

$$Ca_4Al_2(OH)_{12}(H_2O)_4\text{–}Cl_{2(inner)} + SeO_4^{2-} \Leftrightarrow Ca_4Al_2(OH)_{12}(H_2O)_4\text{–}SeO_{4(inner)} + 2Cl^- \quad (2)$$

Since SeO_4^{2-} has a higher affinity for the Friedel phase than Cl^-, the above anion exchanges take place spontaneously. The *in situ* kinetic investigation reveals that the anion exchange first occurs on the LDH particle edges, followed on the basal plane and on the near-surface region, and finally onto the interlayer via diffusion, all within a few minutes [35,36]. Apparently, the surface adsorption/exchange (Eq. (1)) is much more easily taking place, while the exchange within the interlayer anions (Eq. (2)) has to undergo the relevant diffusion and thus encounters a higher energy barrier. Thus, such an adsorption/exchange is a very complicated heterogeneous process, which is the possible reason that the Freundlich model better suits the data points than the Langmuir model (Fig. 5 and Table 2) [15,37]. Freundlich and Langmuir isotherms are normally expressed as follows:

$$Q_e = AC_e^{1/n} \quad (3)$$

$$Q_e = \frac{Q_m b C_e}{1 + bC_e} \quad (4)$$

and the separation factor (R_L) [15,38]

$$R_L = \left(\frac{1}{1 + bC_i}\right) \quad (5)$$

where C_e is the concentration of adsorbate at the equilibrium (mM), C_i the initial concentration of adsorbate (mM), and Q_e the amount of adsorbate adsorbed on the adsorbent (mmol/g). A is the constant in Freundlich isotherm while b and Q_m are the constant and the maximum amount of adsorbate that the adsorbent can adsorb in Langmuir model, respectively. Although the separation factors (R_L = 0.863–0.174) reveal the adsorption is favorable, while the regression is not good (R^2 = 0.835), demonstrating that the adsorbate was not covered in a monolayer and/or the adsorbent surface was not homogeneous. However, the fitting with Freundlich isotherm was much better (R^2 = 0.988), revealing the heterogeneous adsorption in nature. Also n (1.88) indicated that adsorption is favored over the entire range of concentrations, [37,39], consistent with the spontaneous occurrence of SeO_4^{2-} exchange onto the Friedel phase (Eqs. (1) and (2)) due to the higher affinity of SeO_4^{2-} than Cl^-. Furthermore, Dubinin–Radushkevich (D–R) model in Eqs. (6)–(8) was applied to evaluate the free energy of the adsorption process [15]:

$$\ln Q_e = \ln(Q_m) - \beta\varepsilon^2 \quad (6)$$

$$\varepsilon = RT \ln\left(1 + \frac{1}{C_e}\right) \quad (7)$$

$$E = \frac{1}{\sqrt{2\beta}} \quad (8)$$

where Q_e and Q_m are the amount of adsorbate adsorbed on the adsorbent at the equilibrium and the maximum amount that can be adsorbed in D–R model (mmol/g), respectively. E is the free energy of the adsorption process (kJ/mol). As shown in Table 2, the regression using Eq. (6) was good (R^2 = 0.964), and E was 8.75 kJ/mol. This free energy value confirms that adsorption was actually an ion exchange process [15]. In addition, the Temkin isotherm model, taking into consideration the adsorbate/adsorbate interactions on the adsorbent surface, does not exactly describe the selenate adsorption either, indicating such interactions were not the important factor affecting the adsorption.

The XRD patterns of equilibrated selenate-adsorbed AFm at various selenate concentrations are presented in Fig. 6. When [SeO_4^{2-}] is increased from 0.25, to 2.00, and then to 7.60 mM, characteristic diffraction peaks (0 0 3) and (0 0 6) of AFm–Cl (the d-spacing is

Table 2
Langmuir, Freundlich and D–R characteristic constants for selenate adsorption over Friedel phase.

Langmuir				Freundlich			D–R		
Q_m (mmol/g)	b (1/mM)	R_L	R^2	A	n	R^2	Q_m (mmol/g)	E (kJ/mol)	R^2
1.73	0.632	0.863–0.174	0.835	4.38	1.88	0.988	4.27	8.75	0.964

0.781–0.792 nm) are gradually weakened and almost completely disappear at $[SeO_4^{2-}] \geq 2.00$ mM. Simultaneously, a new type of hydrocalumite starts to appear at $[SeO_4^{2-}] = 1.25$ mM, and becomes the dominant phase at $[SeO_4^{2-}] \geq 2.00$ mM, with the d-spacing being 0.962–0.977 nm. The new phase can be assigned to hydrocalumite selenate ($Ca_4Al_2(OH)_{12}SeO_4(H_2O)_4$) and the expansion of the interlayer spacing is due to the intercalation of larger selenate. As estimated from the Se-O bond length, the van der Waal's diameter of SeO_4^{2-} is 0.50 nm, larger than that of Cl^- (0.30 nm), which thus leads to a layer thickness of 0.98 nm, identical to the values observed from the XRD patterns. Note that after selenate exchange, the solution pH is normally increased to ~11 due to the slight dissolution of AFm. As a consequence, the alkaline solution captures some CO_2 from air, which transfers to CO_3^{2-}. The captured carbonate can either intercalate into the AFm interlayer (without the interlayer expansion), or combine with Ca^{2+} to form $CaCO_3$, as reflected by the XRD peak at 29° (Fig. 6). In some cases, the XRD peak of $CaCO_3$ is not obvious, probably due to the good sealing in the experiments so less CO_2 is captured. Thus the influence of carbonate on the selenate adsorption is two-fold: (i) preferable anion exchange and (ii) formation of $CaCO_3$ that may cause some structure change.

Therefore, at a lower concentration, SeO_4^{2-} is mainly adsorbed on the surface and in the near-surface region of Friedel crystallites, resulting in no change of the interlayer spacing. At a higher concentration, more SeO_4^{2-} is intercalated into the interlayer, thus expanding the interlayer and transforming AFm–Cl to selenate-hydrocalumite (AFm–SeO_4).

3.4. Desorption of SeO_4^{2-} from AFm–SeO_4

The selenate in AFm–SeO_4 can be partly recovered through desorption in NaCl solution. Fig. 7 shows the desorption profile of selenate from AFm–SeO_4 as a function of time. The desorption seems fast, reaching equilibrium within the first hour. After 1-h desorption, the desorbed amount does not increase, but rather slightly decreases. Note that the pH jumps to *ca.* 11 when AFm–SeO_4 is added into NaCl solution (initial pH ~7.0). The NaCl concentration affects the desorption of selenate to some degree. In general, the higher the chloride concentration in solution, the larger the amount of selenate desorbed. Fig. 7 shows that 30–50% selenate is desorbed from AFm–SeO_4. Predictably, 60–70% selenate would be desorbed at [NaCl] = 1.0 M. In a case similar to the practical situation, e.g. using 2.0 g/l of AFm–Cl to adsorb selenate from 0.5 mM of SeO_4^{2-} solution (40 ppm Se), we are able to remove >90% selenate from the solution and then recover 70–80% of SeO_4^{2-} from the collected AFm–(Cl,SeO_4) in 0.10 M NaCl solution.

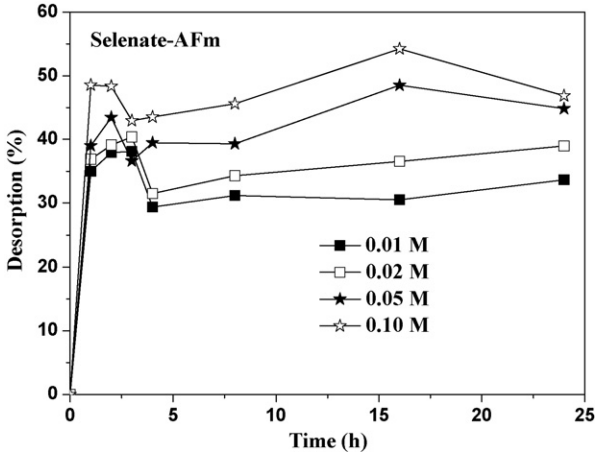

Fig. 7. Desorption profiles of SeO_4^{2-} from pure AFm–SeO_4 material at [NaCl] = 0.01, 0.02, 0.05, and 0.10 M.

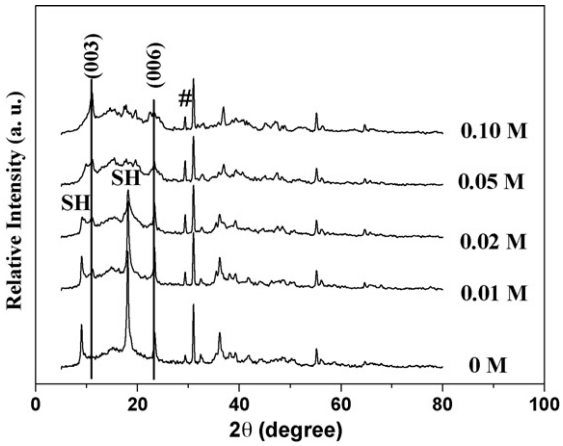

Fig. 8. XRD patterns of SeO_4^{2-} after desorption at [NaCl] = 0, 0.01, 0.02, 0.05 and 0.10 M. SeO_4^{2-} peaks are marked with 'SH', and $CaCO_3$ with '#'.

Similarly, the XRD patterns (Fig. 8) of AFm–SeO_4 after 24-h exchange in various NaCl solutions also reflect the selenate desorption from the interlayer. As shown in Fig. 8 (the bottom curve), all the XRD characteristic peaks of AFm–SeO_4 are kept unchanged after stirring in the pure water for 24 h. With the chloride concentration increasing from 0.01 to 0.10 M, the peaks of AFm–SeO_4 (marked with SH) weaken in intensity. Meanwhile, a new peak at 11° (marked with (0 0 3)) gradually forms, and becomes dominant at $[Cl^-] = 0.10$ M, together with some other minor phases, such as the original AFm–SeO_4 phase and $CaCO_3$ (peak at 29° marked as #). The selenate desorption decreases the layer spacing from 0.977 to 0.778 nm, suggesting the transformation of AFm–SeO_4 to AFm–Cl. This process thus indicates that the Friedel phase could be simply regenerated and reused, and the selenate accumulated on the Friedel phase (AFm–Cl) would be partly recovered for other valuable applications.

3.5. Chemical stability of selenate-adsorbed AFm

The chemical stability of selenate-adsorbed AFm was examined in water with a different initial pH by following the modified TCLP method [31]. The leaching profiles of selenate as a function of time are shown in Fig. 9. The leaching amount at pH 4.00, 7.00 and 10.00 is very small, about 0.001 mmol/g (Se) during the whole leaching period. In comparison with the adsorbed amount of selenate (0.280 mmol/g) in this case, the leaching selenate is only a small

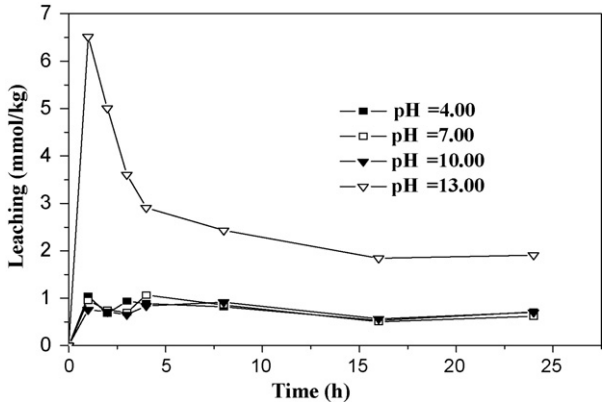

Fig. 9. The leaching profile of SeO_4^{2-} from the selenate-adsorbed Friedel phase (AFm) at pH 4, 7, 10, and 13.

portion (0.3–0.4%) in selenate-adsorbed AFm, showing a high fixation stability of selenate with AFm–Cl. Only at pH 13 does the leaching amount of selenate from selenate-adsorbed AFm increase to 0.0022–0.0065 mmol/g, indicating that even under the severe condition of pH = 13, there is still 97.6–99.2% of SeO_4^{2-} stabilized with the Friedel phase (AFm–Cl).

We observed that the final pH of the leaching solution is 10.70 ± 0.30 when the initial pH is 4.00, 7.00, and 10.00, while it is 11.60 ± 0.30 when the initial pH is 13.00. This means that the Friedel phase has a high neutralization capacity on both acid and alkali media, and thus has a similar exchange capacity of selenate at the different initial pH. The XRD patterns (Supplementary material Fig. 2S) reveals that the Friedel phase is unchanged even at initial pH = 4.0. Presumably, at a lower pH, the framework '$Ca(OH)_2$' is partially dissolved to anti-acidify, leveling pH up to ~11.0. At pH 13.0, the framework '$Al(OH)_3$' is partially dissolved to anti-alkaline, leveling pH down to 11.6. Because more active adsorption site (Al in the layer) is leaching in the latter case, more selenate is thus leached out at the initial pH 13.00.

4. Conclusions

In conclusion, removal of SeO_4^{2-} from an aqueous solution with the Friedel phase (AFm–Cl) is very effective. The removal of SeO_4^{2-} takes place quickly and the isotherm follows the Freundlich model, reflecting heterogeneous adsorption, with the practical removal capacity up to 1.37 mmol(Se)/g at $[SeO_4^{2-}] = 7.60$ mM. The removal occurs via anion exchange as the layer spacing expands from 0.78 to 0.97–0.98 nm when more SeO_4^{2-} is intercalated. The adsorbed selenate can be partially recovered via desorbing in NaCl solution. The TCLP test indicates that selenate–hydrocalumite is chemically stable at pH 4–10. The findings in this research thus demonstrate that the Friedel phase (AFm–Cl), a very environmentally friendly anion-exchanging clay material, is a cost-effective adsorbent for the treatment of SeO_4^{2-}-containing wastewater.

Acknowledgements

This project is supported by National Nature Science Foundation of China No. 20477024, No. 20677037, Shanghai Leading Academic Disciplines (T105). Drs. Xu and Qiao acknowledge the support from the Australian Research Council for the ARC Centre of Excellence for Functional Nanomaterials.

Appendix A. Supplementary data

Supplementary data associated with this article can be found, in the online version, at doi:10.1016/j.jhazmat.2009.11.012.

References

[1] J. Letey, C. Roberts, M. Penberth, C. Vasek, An Agricultural Dilemma: Drainage Water and Toxics Disposal in the San Joaquin Valley, University of California Agricultural Experiment Station, Riverside, CA, 1986.
[2] J. Boegel, D. Clifford, Se oxidation and removal by ion exchange, Report PA/600/2-86/031, U.S. EPA, Washington, DC, 1986.
[3] L. Twidwell, J. Mccloskey, P.E.G.M. Miranda, Potential technologies for removing selenium from process and mine wastewate, site acessado em 07, 2004.
[4] K. Konsult, Modelling of water flow, barrier degradation, chemistry and radionuclide transport in the near field of a repository for L/ILW, Technical Report NTB 88-42, Nagra, Wettingen, Switzerland, 1989.
[5] M.H. Grace, S.B. Robert, Sorption of chromate and other inorganic anions by organo-zeolite, Environ. Sci. Technol. 28 (1994) 452–458.
[6] T. Hongo, T. Iemura, A. Yamazaki, Adsorption ability for several harmful anions and thermal behavior of Zn–Fe layered double hydroxide, J. Ceram. Soc. Jpn. 116 (2008) 192–197.
[7] W.H. Kuan, S.L. Lo, M.K. Wang, Removal of Se(IV) and Se(VI) from water by aluminum-oxide-coated sand, Water Res. 32 (1998) 915–923.
[8] K. Mondal, G. Jegadeesan, S.B. Lalvani, Removal of selenate by Fe and NiFe nanosized particles, Ind. Eng. Chem. Res. 43 (2004) 4922–4934.
[9] T. Nishimura, H. Hashimoto, M. Nakayama, Removal of selenium(VI) from aqueous solution with polyamine-type weakly basic ion exchange resin, Sep. Sci. Technol. 42 (2007) 3155–3167.
[10] A. Walcarius, J. Devoy, J. Bessie're, Interactions of selenate with copper(I) oxide particles, Langmuir 20 (2004) 6335–6343.
[11] T. Yokoi, T. Tatsumi, H. Yoshitake, Fe3+ coordinated to amino-functionalized MCM-41: an adsorbent for the toxic oxyanions with high capacity, resistibility to inhibiting anions, and reusability after a simple treatment, J. Colloid Interface Sci. 274 (2004) 451–457.
[12] Y You, G.F. Vance, H. Zhao, Selenium adsorption on Mg–Al and Zn–Al layered double hydroxides, Appl. Clay Sci. 20 (2001) 13–25.
[13] Y. Zhang, J. Wang, C. Amrhein, W.T. Frankenberger, Removal of selenate from water by zerovalent iron, J. Environ. Qual. 34 (2005) 487–495.
[14] H. Deligöz, M.S. Ak, S. Memon, M. Yilmaz, Azocalixarene. 5: p-substituted azocalix[4]arenes as extractants for dichromate anions, Pak. J. Anal. Environ. Chem. 9 (2008) 1–5.
[15] I.B. Solangi, S. Memon, M.I. Bhanger, Synthesis and application of a highly efficient tetraestercalix[4]arene resin for the removal of Pb2+ from aqueous environment, Anal. Chim. Acta 638 (2009) 146–153.
[16] R. Segni, L. Vieille, F. Leroux, C. Taviot-Guého, Hydrocalumite-type materials: 1. Interest in hazardous waste immobilization, J. Phys. Chem. Solids 67 (2006) 1037–1042.
[17] P.S. Braterman, Z.P. Xu, F. Yarberry, Layered double hydroxides, in: S.M. Auerbach, K.A. Carrado, P.K. Dutta (Eds.), Handbook of Layered Materials, Marcel Dekker, Inc., New York, 2004, pp. 373–474.
[18] T. Kameda, H. Takeuchi, T. Yoshioka, Uptake of heavy metal ions from aqueous solution using Mg–Al layered double hydroxides intercalated with citrate, malate, and tartrate, Sep. Purif. Technol. 62 (2008) 330–336.
[19] J Orthman, H.Y. Zhu, G.Q. Lu, Use of anion clay hydrotalcite to remove coloured organics from aqueous solutions, Sep. Purif. Technol. 31 (2003) 53–59.
[20] I. Baur, C.A. Johnson, The solubility of selenate-Aft ($3CaO{\cdot}Al_2O_3{\cdot}3CaSeO4{\cdot}37.5H_2O$) and selenate–AFm ($3CaO{\cdot}Al_2O_3{\cdot}CaSeO4{\cdot}xH_2O$), Cem. Concr. Res. 33 (2003) 1741–1748.
[21] I. Baur, C.A. Johnson, Sorption of selenite and selenate to cement minerals, Environ. Sci. Technol. 37 (2003) 3442–3447.
[22] I. Bonhoure, I. Baur, Uptake of Se (IV/VI) oxyanions by hardened cement paste and cement minerals: an X-ray absorption spectroscopy study, Cem. Concr. Res. 36 (2006) 91–98.
[23] M. Chrysochoou, D. Dermatas, Evaluation of ettringite and hydrocalumite formation for heavy metal immobilization: Literature review and experimental study, J. Hazard. Mater. 136 (2006) 20–33.
[24] E.A. Johnson, M.J. Rudin, S.M. Steinberg, W.H. Johnson, The sorption of selenite on various formulations, Waste Manag. 20 (2000) 509–516.
[25] D. Peak, D.L. Sparks, Mechanisms of selenate adsorption on iron oxide and hydroxide, Environ. Sci. Technol. 36 (2002) 1460–1466.
[26] R.P.J.J. Rietra, T. Hiemstra, W.H. Riemsdijk, Comparison of selenate and sulfate adsorption on goethite, J. Colloid Interface Sci. 240 (2001) 384–390.
[27] M. Zhang, E.J. Reardon, Removal of B, Cr, Mo, and Se from wastewater by Incorporation into hydrocalumite and ettringite, Environ. Sci. Technol. 37 (2003) 2947–2952.
[28] G.R. Qian, Y.L. Cao, P.C. Chui, J. Tay, Utilization of MSWI fly ash for stabilization/solidification of industrial waste sludge, J. Hazard. Mater. 129 (2006) 274–281.
[29] U.A. Birnin-Yauri, F.P. Glasser, Friedel's salt $Ca_2Al(OH)_6(Cl, OH){\cdot}2H_2O$: its solid solution and their role in chloride binding, Cem. Concr. Res. 28 (1998) 1713–1723.
[30] QuikChem, Method 10-117-07-1-I, Determination of chloride by flow injection analysis colorimetry.
[31] U.S.EPA, in: W. DC (Ed.), Test Methods for Evaluating Solid Waste: Physical/Chemical Methods, Governmental Printing Office, 1986.
[32] M.C. Hermosin, I. Pavlovic, M.A. Ulibarri, J. Cornejo, Hydrotalcites as sorbent for trinitrophenol: sorption capacity and mechanism, Water Res. 30 (1996) 171–177.
[33] D.L. Sparks, Kinetics of Soil Chemical Processes, Academic Press, New York, 1988.
[34] Y. Dai, G.R. Qian, Y. Cao, Y. Xu, J. Zhou, Q. Liu, Z.P. Xu, Effective removal and fixation of Cr(VI) from aqueous solution with Friedel's salt, J. Hazard. Mater. 170 (2009) 1086–1092.
[35] Y.J. Feng, G.R. Williams, F. Leroux, C. Taviot-Gueho, D. O'Hare, Selective anion-exchange properties of second-stage layered double hydroxide heterostructures, Chem. Mater. 18 (2006) 4312–4318.
[36] M.B.J. Roeffaers, B.F. Sels, D. Loos, C. Kohl, K. Mullen, P.A. Jacobs, J. Hofkens, D.E.D. Vos, In situ space- and time-resolved sorption kinetic of anionic dyes on individual LDH crystals, Chem. Phys. Chem. 6 (2005) 2295–2299.
[37] F.H. Frimmel, L. Huber, Influence of humic substances on the adsorption of heavy metals on defined mineral phases, Environ. Int. 22 (1996) 507–517.
[38] G. McKay, H.S. Blair, J.R. Gardner, Adsorption of dyes on chitin. I. Equilibrium studies, J. Appl. Polym. Sci. 27 (1982) 3043–3057.
[39] G. McKay, The removal of color from effluent using various adsorbents-silica, Water Res. 14 (1980) 1–27.
[40] T. Yokoia, T. Tatsumi, H. Yoshitake, Fe3+ coordinated to amino-functionalized MCM-41: an adsorbent for the toxic oxyanions with high capacity, resistibility to inhibiting anions, and reusability after a simple treatment, J. Colloid Interface Sci. 274 (2004) 451–457.